Mutagenesis, 2017, 32, 47–57
doi:10.1093/mutage/gew046
Original Manuscript
Advance Access publication 22 September 2016

OXFORD

Original Manuscript

Surface modification does not influence the genotoxic and inflammatory effects of TiO_2 nanoparticles after pulmonary exposure by instillation in mice

Håkan Wallin[1,2], Zdenka O. Kyjovska[1], Sarah S. Poulsen[1], Nicklas R. Jacobsen[1], Anne T. Saber[1], Stefan Bengtson[1], Petra Jackson[1] and Ulla Vogel[1,3,*]

[1]National Research Centre for the Working Environment, Lersø Parkallé 105, DK-2100 Copenhagen Ø, Denmark, [2]Institute of Public Health, University of Copenhagen, DK-1353 Copenhagen K, Denmark and [3]Department of Micro- and Nanotechnology, Technical University of Denmark, DK-2800 Kgs. Lyngby, Denmark

*To whom correspondence should be addressed. Tel: +45 39 16 52 00; Fax: +45 39 16 52 01; Email: ubv@nrcwe.dk

Received 4 May 2016; Revised 26 August 2016; Accepted 30 August 2016.

Abstract

The influence of surface charge of nanomaterials on toxicological effects is not yet fully understood. We investigated the inflammatory response, the acute phase response and the genotoxic effect of two different titanium dioxide nanoparticles (TiO_2 NPs) following a single intratracheal instillation. NRCWE-001 was unmodified rutile TiO_2 with endogenous negative surface charge, whereas NRCWE-002 was surface modified to be positively charged. C57BL/6J BomTac mice received 18, 54 and 162 μg/mouse and were humanely killed 1, 3 and 28 days post-exposure. Vehicle controls were tested alongside for comparison. The cellular composition and protein concentration were determined in bronchoalveolar lavage (BAL) fluid as markers for an inflammatory response. Pulmonary and systemic genotoxicity was analysed by the alkaline comet assay as DNA strand breaks in BAL cells, lung and liver tissue. The pulmonary and hepatic acute phase response was analysed by *Saa3* mRNA levels in lung tissue or *Saa1* mRNA levels in liver tissue by real-time quantitative polymerase chain reaction. Instillation of NRCWE-001 and -002 both induced a dose-dependent neutrophil influx into the lung lining fluid and *Saa3* mRNA levels in lung tissue at all assessed time points. There was no statistically significant difference between NRCWE-001 and NRCWE-002. Exposure to both TiO_2 NPs induced increased levels of DNA strand breaks in lung tissue at all doses 1 and 28 days post-exposure and NRCWE-002 at the low and middle dose 3 days post-exposure. The DNA strand break levels were statistically significantly different for NRCWE-001 and -002 for liver and for BAL cells, but no consistent pattern was observed. In conclusion, functionalisation of reactive negatively charged rutile TiO_2 to positively charged did not consistently influence pulmonary toxicity of the studied TiO_2 NPs.

Introduction

Titanium dioxide (TiO_2) is one of the most commonly produced and widely used nanoparticles (NPs). The nanosized form has a wide range of uses such as an ultraviolet (UV) filter in cosmetics and lacquers, and aggregated or agglomerated nanosized and micronsized forms are the most commonly used white pigment in paints, paper, plastics, toothpaste, pharmaceuticals, candy and food. TiO_2 particles are considered insoluble and chemically stable, but as the particle size is reduced, they become more reactive (1–3) and they are also used as for catalysts, especially in combination with UV light.

© The Author 2016. Published by Oxford University Press on behalf of The UK Environmental Mutagen Society.
This is an Open Access article distributed under the terms of the Creative Commons Attribution Non-Commercial License (http://creativecommons.org/licenses/by-nc/4.0/), which permits non-commercial re-use, distribution, and reproduction in any medium, provided the original work is properly cited. For commercial re-use, please contact journals.permissions@oup.com

Inhalation of nanosized TiO_2 particles may potentially cause adverse health effects in exposed workers and consumers (4). TiO_2 is classified by the International Agency for Research on Cancer (IARC) as being possible carcinogen to humans by inhalation (Group 2B), based on sufficient evidence in experimental animals and inadequate (little) evidence from epidemiological studies (5), and the European Chemicals Agency recently opened for commenting a proposition for classifying TiO_2 as a carcinogen (Carc 1B) in Europe (available at: https://www.paint.org/echa-releases-french-dossier-titanium-dioxide-public-comment/). There is, however, no conclusive evidence of TiO_2-related cancer after the occupational exposure (6,7), and it has been proposed that it is carcinogenic only after massive prolonged inhalation exposure. The National Institute for Occupational Safety and Health (NIOSH) has proposed an occupational exposure limit of 0.3 mg/m^3 for ultrafine TiO_2 particles (8), compared with the current occupational exposure limit of 10 mg/m^3 TiO_2 or 6 mg/m^3 titanium (Ti) in Denmark (available at: http://arbejdstilsynet.dk/da/regler/at-vejledninger/g/c-0-1-graensevaerdi-for-stoffer-og-mat).

Inhaled NPs deposit in the deep respiratory tract and have been shown to remain in the lung for long times (9–12). In the occupational settings, lung is a primary target organ of NP exposure. Airway exposure (inhalation as well as pulmonary instillation) to TiO_2 NPs has been reported to cause inflammation, pulmonary damage, plaque progression and DNA damage in rodents (1–3,10,13–18). Intratracheally instilled TiO_2 NPs are engulfed by pulmonary macrophages, translocate at a low rate and accumulate primarily in the liver, but also in other organs such as heart, kidney, placenta and brain (9–11,19,20). The translocation is very limited and represents less than 1% of the initial pulmonary burden at 1 week post exposure (19). The toxicology of TiO_2 NPs exposure was recently reviewed by Shi et al. (21).

To facilitate hazard assessment of nanomaterials (NMs), it is important to identify the physico-chemical properties of NMs that predict adverse outcomes. The total surface area of deposited NPs seems to be an important predictor of pulmonary inflammation and acute phase response (3,22–24). The role of surface modification and surface charge is less clear (3).

The purpose of this study was to compare the inflammatory and genotoxic effects of two types of TiO_2 NPs with different surface charge after intratracheal instillation (i.t.) in mice. The adverse effects were determined 1, 3 and 28 days post-exposure. The chosen doses correspond to the estimated pulmonary deposition during 1.5, 5 and 15 working days at the current Danish occupational exposure level for TiO_2 (10 mg/m^3) assuming 9% alveolar deposition and a ventilation rate of 1.8 l/h (9,14). Inflammation was determined as the influx of inflammatory cells in the lung lining fluid [by the cellular composition in the bronchoalveolar lavage (BAL) fluid (BALF)], and BALF protein concentration was assessed as a general marker of lung tissue damage. *Saa3* mRNA levels in lung and *Saa1* levels in liver were used as biomarkers for acute phase response (24–26). Genotoxicity was assessed as DNA strand breaks determined by comet assay in BAL cells, lung and liver. The biological markers and time points were chosen to enable comparison of adverse health effect with other NPs tested in our lab with the same set-up and increase knowledge of prediction the adverse effects of other NMs (2,10,15,17,25–31).

Materials and methods

Mice

Female mice C57BL/6J BomTac aged 6–7 weeks were obtained from Taconic Europe (Ejby, Denmark). Mice were allocated randomly to the experimental groups and were acclimatized for 1–2 weeks before the start of experiment. The caging conditions were as previously described in detail (32). Briefly, all mice were housed in polypropylene cages with bedding (sawdust) and activity enrichment at controlled environmental conditions; temperature (21 ± 1°C), humidity (50 ± 10%) and 12 h light/dark period. Mice had access to food (Altromin 1324) and tap water *ad libitum*. The animals were assigned to i.t. at 8 weeks of age. The average weight at the day of instillation was 18.5 ± 1.3 g. All procedures complied with the EC Directive 86/609/EEC and Danish law regulating experiments with animals (The Danish Ministry of Justice, Animal Experiments Inspectorate, permission 2010/561–1779).

Study design

Mice were intratracheally instilled with a single dose of vehicle (Nanopure water), and two different TiO_2 NPs NRCWE-001 and NRCWE-002 in doses: 18, 54 or 162 µg/mouse, mice were killed after 1, 3 or 28 days. The chosen doses correspond to 1.5, 5 and 15 working days at the Danish occupational exposure level for TiO_2 (6.0 mg Ti/m^3–10 mg TiO_2/m^3), respectively. NPs groups consisted of 8 mice for each dose and time point, and the vehicle control group consisted of 12 mice for each time point. The organs and BAL were collected 1, 3 and 28 days post-exposure. A total of 180 mice were used in this study. Data on the vehicle controls have been published previously (30).

Particle characterisation and preparation of exposure stock

In this study, two rutile TiO_2 NPs (NRCWE-001 and NRCWE-002) were used. NRCWE-001 particle was purchased from NanoAmor (Houston, TX, USA) and used for production of NRCWE-00NRCWE-002 (positively charged; amino-TiO_2) at the National Research Center for Working Environment (33). The NRCWE-002 was surface functionalised by 3-aminopropyltriethoxysilane (purity 99%, Sigma-Aldrich, Glostrup, Denamark). The zeta potential of NRCWE-001 was –36.8 mV at pH 7.22, –26 mV at pH 7.0 and –7.2 mV at pH 4.4 and for NRCWE-002 was 35.4 mV at pH 7.4, 25 mV at pH 7.0 and 20.4 mV at pH 4.4 (all in about 1 mM sodium phosphate buffer). A detailed description of the preparation was reported previously (34). Both particles have 10 nm declared primary particle sizes, the Brunauer–Emmett–Teller (BET) analysis (BET) surface area for NRCWE-001 is 99 m^2/g and 84 m^2/g for NRCWE-002, respectively (3,34).

NPs were suspended in 0.2 µm filtered, γ-irradiated Nanopure Diamond UV water (Pyrogens: <0.001 EU/ml, total organic carbon: <3.0 ppb) and sonicated on ice, for 16 min without pause, using a Branson Sonifier S-450D (Branson Ultrasonics Corp., Danbury, CT, USA) equipped with a disruptor horn (model number 101-147-037). The desired concentrations were 18, 54 and 162 µg/instillation. The 3.24 mg/ml (162 µg/instillation) suspension was subsequently diluted 1:3 to obtain 1.08 mg/ml (54 µg/instillation) and diluted further 1:3 for the lowest dose 0.36 mg/ml (18 µg/instillation). Each of these dilutions were sonicated for extra 2 min before instillation. Vehicle was prepared by sonication of Nanopure Diamond water in the same conditions and duration (16 min) as described above. All suspensions were freshly made for the instillation and were only used for up to 1 h post preparation.

Dynamic light scattering

The hydrodynamic size distributions in suspensions were determined by dynamic light scattering (DLS) using Malvern Zetasizer Nano ZS (Malvern Instruments Ltd, UK). Data were analysed on Dispersion

Technology Software v5.0 (Malvern Instruments Ltd). The size distribution was determined directly after sonication on the instillation dispersions at 25°C in 1 ml disposable polystyrene cuvettes. All data were obtained based on six consecutively repeated analyses of the same sample with no pause. For calculation of hydrodynamic size, we used the refractive (R_i) and absorption indices (R_s) of 2.903 and 0.10, respectively, for both rutile TiO_2 NPs and standard optical and viscosity properties for H_2O.

Particle exposure by i.t.

Eight-week-old female mice were once instilled intratracheally under isofluorane sedation as previously described (35). Briefly, mice were anaesthetized with 4% isofluorane and instilled through the trachea with vehicle or TiO_2 NPs dispersed in vehicle (50 µl solution followed by 200 µl air). The total instilled doses were 18, 54 and 162 µg/mouse. After instillation, the mice were weighed and transferred to the home cage until termination.

BAL preparation and isolation of organs

Upon termination, mice were anaesthetized using Hypnorm® (fentanyl citrate 0.315 mg/ml and fluanisone 10 mg/ml from Janssen Pharma) and Dormicum® (Midazolam 5 mg/mL from Roche). Both anaesthetics were mixed with equal volumes of sterile water. Heart blood was withdrawn. Lungs were flushed twice with sterile 0.9% sodium chloride (NaCl) through the trachea to obtain BALF. The volume used for each flush was calculated as 1 ml 0.9% NaCl/25 g mouse weight and varied from 0.7 to 0.9 ml. The BALF was stored on ice until centrifugation at 400 × *g* for 10 min at 4°C. Acellular BALF was recovered and stored at –80°C. The BAL cells were resuspended in 100 µl medium (HAM F-12 with 1% penicillin/streptomycin and 10% fetal bovine serum).

The total number of living and dead cells in BAL was determined by NucleoCounter NC-200TM (Chemometec, Denmark) from 20 µl diluted cell suspension following manufacturer's protocol. Samples for COMET assay were prepared from 40 µl resuspended BAL cells and 60 µl freezing media (HAM F-12, 1% penicillin/streptomycin, 15% fetal bovine serum and 10% dimethyl sulphoxide). Samples were divided into two aliquots of 50 µl each and immediately frozen at –80°C. The rest of cell resuspension (40 µl) was used to determine cell composition. The cell suspension was centrifuged at 55 × *g* for 4 min in Cytofuge 2 (StatSpin, TRIOLAB, Brøndby, Denmark) on to a microscope glass slide and then fixed for 5 min in 96% ethanol. All slides were stained with May-Grünwald-Giemsa, randomised and blinded, before counting 200 cells/sample under light microscope (100× magnification, immersion oil). Lung and liver tissues were divided into four parts, snap frozen in liquid nitrogen, and stored at –80°C.

Comet assay: preparation and analyses

DNA strand breaks were determined on frozen BAL cells suspension, lung (3 × 3 mm of left lobe) and liver tissue (3 × 3 mm piece of the median lobe). Sample preparation and comet analysis has previously been described in detail (36). Briefly, BAL cells, lung or liver cell suspensions, were embedded in agarose (0.7% final concentration) on Trevigen 20-Well CometSlides™. Slides were quickly immersed into lysing solution at 4°C and stored overnight. On the next day, samples were alkaline treated and subjected to alkaline electrophoresis in ice-cold circulating electrophoresis solution (25 min, 1.15 V/cm, pH >13). Samples were neutralised, fixed and later stained by SYBRGreen®. Comets were scored by the fully automated PathFinder™ system (IMSTAR, France). DNA strand breaks were quantified as %DNA in the comet tail (%TDNA) and the comet tail length (TL). The day-to-day variation and electrophoresis efficiency was controlled by including phosphate-buffered saline exposed and 60 µM hydrogen peroxide-exposed A549 cells as negative and positive controls, respectively, on all comet slides. Control cells were exposed for 30 min at 4°C as described (36). The day-to-day variation for the comet assay analysis on BAL, lung and liver tissue (n = 19 for each tissue) were 19.3%, 13.1% and 16.7%, for TL, respectively.

Total protein concentration in BALF

Total protein content in BALF was measured by Pierce®BCA Protein Assay Kit (Thermo Scientific, USA) according to the manufacturer's protocol. Briefly, protein concentration of all unknown acellular BALF samples were compared to a standard curve of known albumin concentrations. Samples were prepared in duplicates and were incubated 30 min in 37°C. Absorbance was measured at 550 nm on Victor Wallac 1420 Multilabel counter (Turku, Finland).

Saa mRNA expression analysis

RNA from right lung (16–20 mg) and liver (a sample of 15–25 mg) was isolated using Maxwell® 16 LEV simply RNA Tissue Kit (AS1280, Promega, USA) according to the manufacturer's protocol. RNA was eluted by 50 µl nuclease-free (DEPC) water. cDNA was prepared from DNAse-treated RNA using Taq-Man® reverse transcription reagents (Applied Biosystems, USA) as described by manufacturer's protocol. Total RNA and cDNA concentration was measured on NanoDrop 2000c (ThermoFisher, USA). The *Saa3* and *Saa1* gene expression was determined using real-time reverse transciptase polymerase chain reaction (RT-PCR) with 18S RNA as reference gene as previously described (23,37). In brief, each sample was run in triplicates on the ViiA7 Real-Time PCR (Applied Biosystems, USA). In all assays, TaqMan predeveloped master mix (Applied Biosystems, USA) was used. Target and 18S RNA levels were quantified in triplicates in separate wells. The relative expression of the target gene was calculated by the comparative method $2^{-\Delta C_t}$. mRNA measurements were excluded if the 18S RNA content fell outside the linear range in which the PCR was found to be quantitative defined by the validation experiments. Negative controls, where RNA had not been converted to cDNA (no template control), were included in each run. A plate control was included in all real-rime RT-PCR analyses. The sequences of the *Saa3* primers and probe were: *Saa3*-forward: 5′ GCC TGG GCT GCT AAA GTC AT 3′, *Saa3*-reverse: 5′ TGC TCC ATG TCC CGT GAA C 3′ and *Saa3*-probe: 5′ FAM-TCT GAA CAG CCT CTC TGG CAT CGC T-TAMRA 3′.The day-to-day variation for the plate control in the *Saa3* analyses was 9.9 %. For *Saa1* expression analyses, a primer/probe mix was used (Assay ID: Mm00656927_g1, ThermoFisher Scientific, USA). The day-to-day variation for the plate control in the *Saa1* analyses was 11.9%.

Statistical analyses

The experimental data were transformed by logarithmic transformation (comet assay, protein concentration and *Saa3* and *Saa1* mRNA level) or ranked (BAL cell composition) and analysed by two-way analysis of variance (ANOVA). If statistical significance was reached in the overall ANOVA test (dose and time were used as categorical parameters), a post hoc Tukey-type multiple comparison test was used. If the interaction was significant, one-way ANOVA was performed with post hoc Tukey-type multiple comparison test. The relevant particle differences were tested by one-way ANOVA, where surface modification was used as categorical value. Statistical

significances were tested at $P < 0.05$ level. All data in the article and tables are expressed as mean ± SEM. The statistical analyses were performed in MiniTab®15.1.0.0 (MiniTab Inc., UK), with the exception of *Saa1* expression analyses, which were performed in SAS version 9.3 (SAS Institute Inc., Cary, NC, USA).

Results

Particle characterisation

All NPs were dispersed in Nanopure water. Size distributions were measured by DLS and are summarized in the Table 1. Unmodified nanoparticle NRCWE-001 shows identical properties at all concentrations. Agglomerates were smaller than 100 nm, at all concentrations; the final suspensions appeared dispersed, stable and we did not observe large aggregates. The positively charged NRCWE-002 formed larger agglomerates, and the agglomerate size varied between 1281 nm (0.36 mg/ml) and 1718 nm (3.24 mg/ml; Figure 1).

Mouse weight

Mice exposed to NRCWE-001 had a weight gain similar to vehicle controls. Body weight of the NRCWE 002-exposed mice was unaffected by instillation 1 and 3 days post-exposure. Mice had dose dependently lower weight gain 28 days after exposure to NRCWE-002 compared with vehicle-exposed mice ($P < 0.001$; data not shown).

BALF cell composition

Recruitment of inflammatory cells in BALF was assessed as a marker of pulmonary inflammation (Table 2).

The total number of cells in BALF was statistically significantly increased 1 and 3 days post-exposure for both TiO_2 NPs compared with the vehicle control ($P < 0.001$) and at day 28 for NRCWE-001. There was no statistically significant difference in total BAL cell numbers between the two TiO_2 NPs.

For both TiO_2 NPs, dose-dependent neutrophil influx was observed 1 day, 3 days and 28 days post-exposure. Exposure to the lowest dose of 18 µg TiO_2 NPs did not affect neutrophil recruitment into lung at any studied time point.

The number of macrophages in BALF was statistically significantly decreased 1 day following exposure to the highest dose of NRCWE-001. The number of macrophages increased over time after instillation and at day 28, the number of macrophages was increased 2.1-fold compared with vehicle controls for the highest dose ($P < 0.001$) for NRCWE-001. The number of macrophages in BAL compared with vehicle controls was unaffected by i.t. exposure to NRCWE-002 at all doses. At post-exposure Day 3, a statistically significantly increased number of eosinophils was observed after exposure to the highest dose of both TiO_2 NPs and the middle dose of NRCWE-002. The number of lymphocytes was increased for the middle and highest dose 28 days post-exposure NRCWE-002 compared with vehicle controls.

The inflammatory response was dose dependent, and we did not observe any statistically significant differences between NRCWE-001 and NRCWE-002.

Successful delivery of TiO_2 NP to the lung was confirmed by the presence of particles in BALF from all exposed mice (results not shown). TiO_2 NPs were observed outside as well as inside macrophages. The number of free as well as engulfed particles decreased in time, but both TiO_2 NPs were still observed 28 days post-exposure (results not shown) as previously reported for other NPs (10,30).

Table 1. Size distributions measure by dynamic light scattering for NRCWE-001 and NRCWE-002

NM	NRCWE-001			NRCWE-002		
Dose	18	54	162	18	54	162
Z-Average (d.nm)	107	107	108	1718	1977	1898
Pd	0.14	0.14	0.15	0.36	0.32	0.16
Hydrodynamic peak size	50.8	21 and 58.5	68.1	1281	1484	1718

DNA strand breaks

Genotoxicity was evaluated as alkali-labile sites and DNA strand breaks by the comet assay in BAL cells, lung and liver tissue (Table 3; Figure 2).

Overall, significantly increased levels of DNA strand breaks assessed as TL were observed in the lung tissue 1 day after exposure to all NRCWE-001 and all NRCWE-002 doses (Figure 2). DNA strand break levels expressed as %TDNA were only statistically significantly increased for the dose 54 µg NRCWE-002 ($P < 0.01$). However, there was the same tendency as observed for TL. On post-exposure Day 3, increased DNA strand break levels were observed for the two lower doses of NRCWE-002 when assessed as TL and for the lowest dose when assessed as %DNA. DNA strand break levels expressed as both TL and %DNA were increased for all NP-exposed mice 28 days post-exposure for all doses, compared with the vehicle controls ($P < 0.001$). Pearson's correlation coefficient between %TDNA and TL in lung cells including all tested samples was $R^2 = 0.76$ (results not shown).

The DNA strand break levels in BAL cells were lowered after exposure to NRCWE-002 1 day post-exposure (TL; $P < 0.001$; Table 3). Three days post-exposure, NRCWE-001 statistically significantly increased the level of TL for low and middle doses and NRCWE-002 exposure led to increased DNA strand break levels at the highest dose compared with the vehicle controls (1.3-fold; $P < 0.001$). Pearson's correlation coefficient between TL and %TDNA in BAL cells was $R^2 = 0.47$ (data not shown).

The DNA strand break levels in liver cells were statistically significantly increased 1 day after exposure to NRCWE-002 expressed as %DNA (Table 3). Increased DNA strand break levels were observed for the highest dose of NRCWE-001 3 days post-exposure and for lowest and the highest dose of NRCWE-001 28 days post-exposure. Pearson's correlation coefficient between %TDNA and TL in liver cells was $R^2 = 0.62$.

There was statistically significant difference between the genotoxic response in liver at the Day 1 ($P < 0.01$) and overall in BAL cells ($P < 0.05$) after i.t. exposure to NRCWE-001 and NRCWE-002. There was no statistically significant difference between the genotoxic responses to NRCWE-001 and NRCWE-002 in lung tissue.

Total protein in BALF

Protein content in BALF was assessed as a marker of increased membrane permeability due to cell damage (Figure 3). The highest dose of NRCWE-001 significantly increased the protein concentration in BALF ($P < 0.05$) at all three post-exposure days. The protein concentration in BALF was unaffected by NRCWE-002 exposure. Overall, there was no statistically significant difference between the two studied NPs.

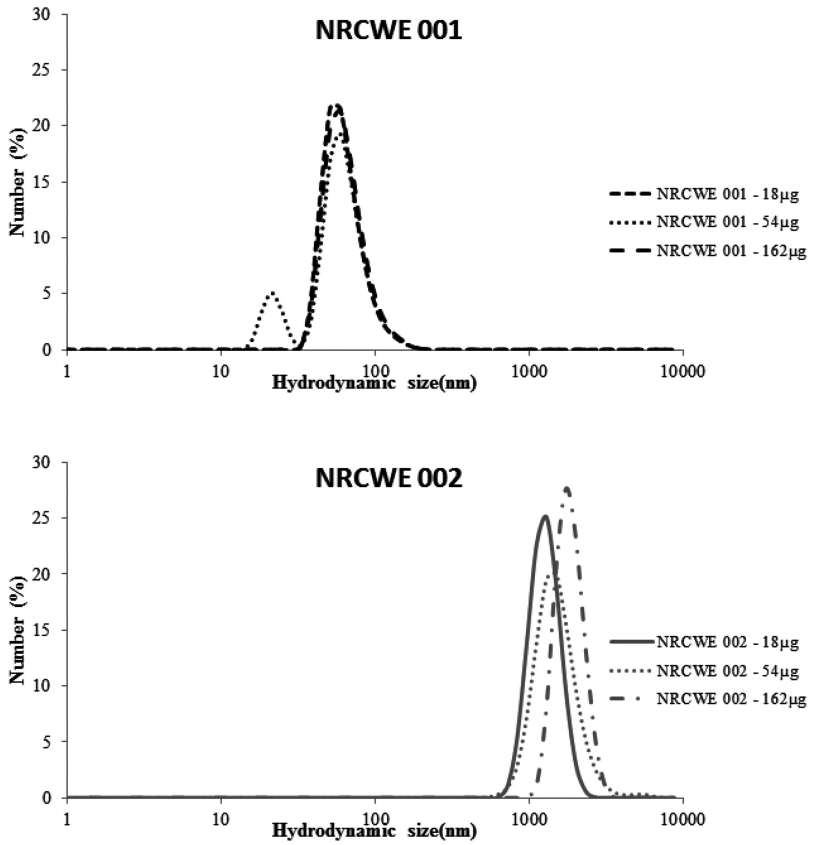

Figure 1. Dynamic light scattering analysis of NRCWE-001 (top panel) and NRCWE-002 (bottom panel) in instillation medium (Nanopure water).

Table 2. Total cell counts from BALF and cells distribution by cells type 1, 3 and 28 days post-exposure to NRCWE 001, NRCWE 002 and vehicle (particle exposed groups $n = 8$, vehicle group $n = 12$)

	Vehicle	NRCWE 001			NRCWE 002		
	0 µg	18 µg	54 µg	162 µg	18 µg	54 µg	162 µg
Day 1							
Group	1	2	3	4	5	6	7
Neutrophils	6.3 ± 1.8	13.2 ± 2.5	90.1 ± 5.4**	183.7 ± 20.6***	9.7 ± 2.2	90.4 ± 15.4**	118.2 ± 9.6***
Macrophages	54.9 ± 3.5	53.2 ± 5.3	54.6 ± 4.7	36.3 ± 4.3*	83.6 ± 6.7	36.8 ± 3.9	50.5 ± 6.7
Eosinophils	1.7 ± 1.0	0.1 ± 0.1*	5.7 ± 1.7	1.5 ± 0.6	0.3 ± 0.2	3.3 ± 1.4	4.6 ± 1.9*
Lymphocytes	0.8 ± 0.5	0.2 ± 0.1	0.5 ± 0.2	0.0 ± 0.0	0.3 ± 0.2	0.2 ± 0.1	0.1 ± 0.2
Epithelial	18.8 ± 2.4	12.0 ± 1.8	10.3 ± 0.6*	6.7 ± 1.2**	24.0 ± 3.9	12.4 ± 2.6	10.6 ± 1.2
Total BAL cells	70.0 ± 9.6	78.9 ± 8.7	161.3 ± 9.8***	228.1 ± 23.1***	117.8 ± 8.9	143.0 ± 14.8**	184.0 ± 13.9***
Day 3	9	10	11	12	13	14	15
Neutrophils	0.4 ± 0.1	3.2 ± 1.9	19.4 ± 4.7***	92.6 ± 15.3***	2.2 ± 0.9	28.0 ± 8.5***	78.3 ± 11.8***
Macrophages	55.5 ± 8.9	60.5 ± 11.7	70.2 ± 7.8	93.6 ± 15.2	66.9 ± 7.9	92.8 ± 13.5	90.6 ± 12.5
Eosinophils	0.3 ± 0.1	0.6 ± 0.4	6.2 ± 2.0	10.0 ± 3.1***	0.9 ± 0.4	7.1 ± 4.7***	10.2 ± 2.9***
Lymphocytes	0.3 ± 0.1	0.0 ± 0.0	0.6 ± 0.3	6.0 ± 1.6	0.9 ± 0.3	1.9 ± 1.1	2.9 ± 1.1*
Epithelial	13.9 ± 2.8	10.6 ± 1.8	12.4 ± 3.3	12.8 ± 2.0*	16.2 ± 3.2	15.6 ± 1.9	21.0 ± 4.2
Total BAL cells	70.4 ± 11.1	74.9 ± 14.9	108.8 ± 13.1	215.0 ± 12.6***	87.1 ± 9.1	145.5 ± 21.2**	203.1 ± 23.2***
Day 28	17	18	19	20	21	22	23
Neutrophils	0.5 ± 0.2	1.2 ± 0.5	2.2 ± 0.7	9.9 ± 2.0***	0.4 ± 0.4	5.4 ± 1.9**	8.3 ± 3.7**
Macrophages	58.3 ± 7.9	87.1 ± 12.4	94.9 ± 15.6	121.8 ± 22.4*	48.7 ± 9.4	62.9 ± 4.5	61.3 ± 10.3
Eosinophils	1.1 ± 1.0	1.4 ± 1.3	1.1 ± 0.9	0.2 ± 0.2	0.1 ± 0.1	1.4 ± 0.7	0.6 ± 0.5
Lymphocytes	0.5 ± 0.3	1.6 ± 0.6	1.0 ± 0.6	2.9 ± 1.7	0.1 ± 0.1	4.0 ± 1.0***	4.0 ± 1.8***
Epithelial	11.1 ± 2.0	9.9 ± 0.9	11.2 ± 2.0	17.9 ± 3.7	13.5 ± 3.9	12.7 ± 1.6	16.1 ± 2.6
Total BAL cells	71.4 ± 8.6	101.2 ± 12.5	110.3 ± 16.5	152.7 ± 24.1**	71.8 ± 10.2	86.2 ± 4.7	90.4 ± 15.7

Mean ± SEM ($\times 10^3$), $^*P < 0.05$, $^{**}P < 0.01$, $^{***}P < 0.001$ cells influx in diesel exhaust particle-treated group vs. vehicle controls, respectively.

Table 3. Summary of comet assay results from BAL cells, lung and liver tissue 1, 3 and 28 days post-exposure to vehicle, NRCWE-001 and NRCWE-002 (vehicle group $n = 12$, particle-exposed groups $n = 8$)

		Vehicle	NRCWE-001			NRCWE-002		
	Dose	0 µg	18 µg	54 µg	162 µg	18 µg	54 µg	162 µg
1 day								
	BAL TL	14.3 ± 0.6	12.7 ± 0.7	14.3 ± 0.5	14.1 ± 0.5	10.0 ± 0.5***	9.7 ± 0.5***	9.4 ± 0.5***
	BAL %TDNA	4.6 ± 0.4	4.2 ± 0.3	3.9 ± 0.3	3.7 ± 0.3	3.9 ± 0.6	4.2 ± 0.4	4.0 ± 0.4
	Lung TL	9.9 ± 0.4	13.2 ± 1.1**	13.5 ± 0.8**	13.1 ± 0.4**	13.7 ± 0.4***	17.9 ± 0.5***	16.2 ± 0.7***
	Lung %TDNA	3.8 ± 0.3	4.5 ± 1.0	4.4 ± 0.5	3.6 ± 0.3	3.2 ± 0.3	5.6 ± 0.4**	4.9 ± 0.5
	Liver TL	16.3 ± 1.4	18.2 ± 0.5	14.7 ± 0.5	15.2 ± 0.8	19.3 ± 1.8	20.2 ± 1.5	20.3 ± 1.8
	Liver %TDNA	4.5 ± 0.5	4.3 ± 0.3	4.1 ± 0.2	4.1 ± 0.4	6.6 ± 1.0*	7.0 ± 0.7*	6.2 ± 0.8*
3 days								
	BAL TL	12.7 ± 0.7	16.1 ± 0.4***	16.6 ± 0.5***	14.2 ± 0.3	9.2 ± 0.2*	15.8 ± 1.1	16.1 ± 1.1*
	BAL % TDNA	5.1 ± 0.4	5.9 ± 0.7	6.2 ± 0.4	5.2 ± 0.3	4.4 ± 0.4	6.2 ± 0.5	7.4 ± 0.7*
	Lung TL	10.7 ± 0.6	12.3 ± 0.4	12.0 ± 0.4	12.2 ± 0.5	13.2 ± 0.7**	12.9 ± 0.2*	12.3 ± 0.5
	Lung %TDNA	2.1 ± 0.4	3.3 ± 1.3	2.7 ± 0.2	2.8 ± 0.3	3.7 ± 1.8**	3.2 ± 0.2	3.1 ± 0.3
	Liver TL	18.2 ± 1.4	15.3 ± 1.1	14.1 ± 0.6	21.8 ± 0.9	21.0 ± 2.1	18.8 ± 0.4	18.7 ± 0.7
	Liver %TDNA	4.5 ± 0.5	3.6 ± 0.4	4.0 ± 0.3	7.2 ± 0.5**	6.9 ± 1.1	5.7 ± 0.3	5.8 ± 0.4
28 days								
	BAL TL	13.9 ± 0.7	14.3 ± 0.7	12.8 ± 0.8	12.4 ± 0.3	15.1 ± 1.1	15.3 ± 1.2	13.7 ± 0.9
	BAL %TDNA	4.8 ± 0.5	5.2 ± 0.6	4.1 ± 0.5	4.2 ± 0.4	6.4 ± 0.8	5.1 ± 0.7	4.6 ± 0.5
	Lung TL	9.1 ± 0.4	16.1 ± 0.9***	17.0 ± 0.9***	15.4 ± 0.8***	16.0 ± 0.5***	15.4 ± 0.5***	15.3 ± 1.3***
	Lung %TDNA	2.0 ± 0.4	5.0 ± 0.7**	6.5 ± 0.7***	5.7 ± 0.5***	5.0 ± 0.3**	5.2 ± 0.4**	5.9 ± 1.0***
	Liver TL	18.4 ± 1.1	23.1 ± 1.2**	21.4 ± 0.5	24.3 ± 0.9**	18.5 ± 0.5	19.7 ± 0.8	17.9 ± 1.0
	Liver %TDNA	5.7 ± 0.6	9.3 ± 1.1**	5.8 ± 0.4	7.7 ± 0.6	5.6 ± 0.4	6.2 ± 0.6	6.0 ± 0.6

Mean ± SEM. $*P < 0.05$, $**P < 0.01$, $***P < 0.001$: using non-parametric two-way ANOVA with post hoc Tukey-type multiple comparison test with time after exposure and dose as categorical variables.

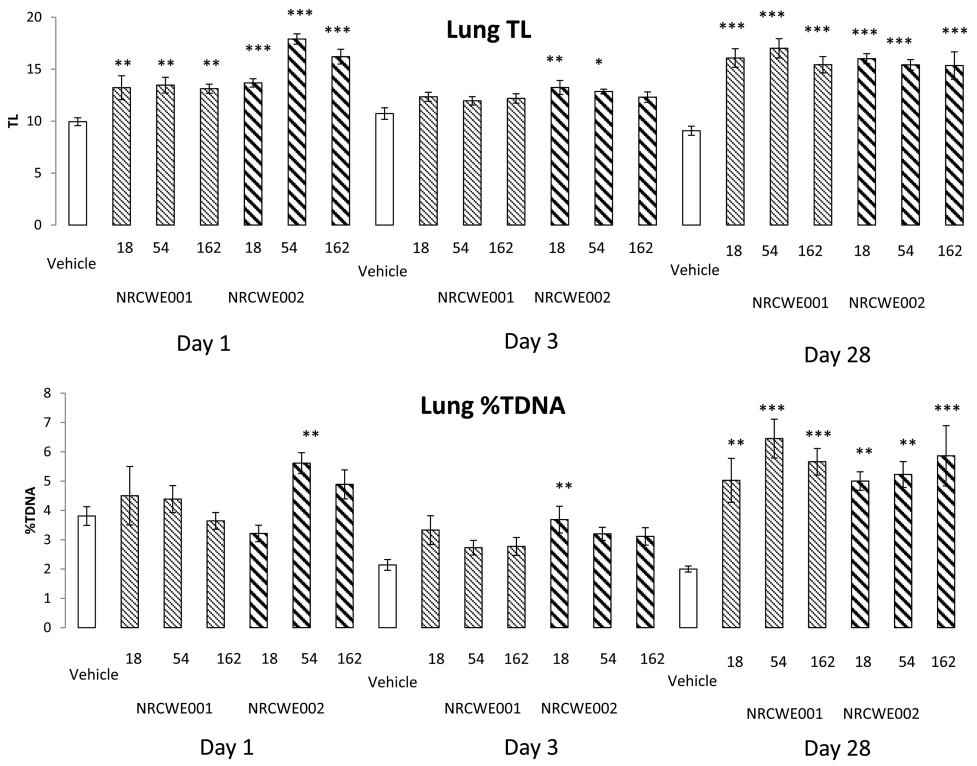

Figure 2. Levels of DNA strand breaks in lung tissue from mice 1, 3 and 28 days after intratracheal instillation of NRCWE-001 and NRCWE-002. Levels of DNA strand breaks was measured by comet assay: (**A**) data shown as tail length (TL) and (**B**) data shown as %DNA in tail (%TDNA). The values represent single mouse measurement in three different post-exposure times (1, 3 and 28 days) after single administration of NRCWE-001 and NRCWE-002 (18, 54, 162 µg/animal) and vehicle controls. The values represent mean of all animals in the group ± SEM ($n = 8$–12). $*P < 0.05$, $**P < 0.01$, $***P < 0.001$: TL and %TDNA, respectively, in NRCWE-001 and NRCWE-002–treated group vs. vehicle controls.

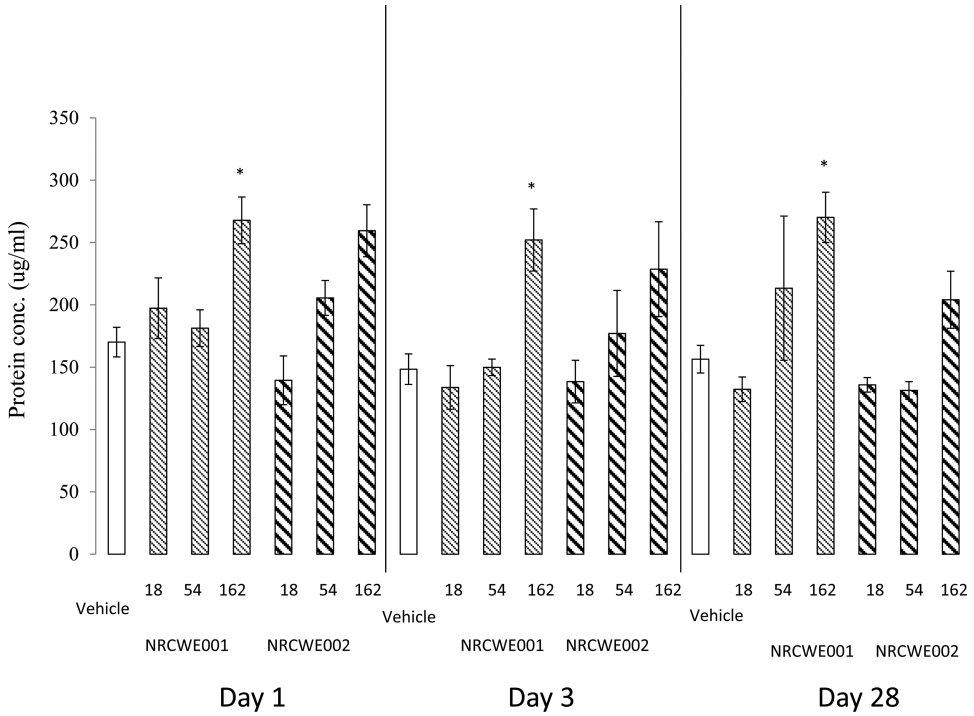

Figure 3. Total protein concentration in BALF with dose response effect in mice 1, 3 and 28 days after intratracheal (i.t.) instillation of NRCWE-001 and NRCWE-002. Female mice were treated by a single dose i.t. of NRCWE-001, NRCWE-002 in three different concentrations (18, 54, 162 µg/mouse), or vehicle, and the mice were killed 1, 3 and 28 days post-exposure. The values represent mean of all animals in the group ± SEM (n = 8–12). *P < 0.05: protein concentration in NRCWE-001 and NRCWE-002–treated group vs. vehicle controls.

Saa mRNA expression

Pulmonary *Saa3* mRNA levels were used as a biomarker of pulmonary acute phase response (23,24), and hepatic *Saa1* mRNA levels were used as biomarker of hepatic acute phase response (25,37).

Pulmonary *Saa3* mRNA expression levels were statistically significantly increased at all three time points following instillation of 162 µg NCRWE 001 and -002 NPs (P < 0.001; Figure 4). The expression levels of *Saa3* mRNA were highest at Day 1. At 1 and 28 days post-exposure, *Saa3* mRNA expression levels were also increased for the middle dose of NRCWE-002 (P < 0.001). No other time or dose-related changes in pulmonary *Saa3* expression levels were observed. There was a strong correlation between specific surface area (BET) and level of pulmonary *Saa3* mRNA expression 1 day post-exposure (NRCWE-001 R^2 = 0.57 and NRCWE-002 R^2 = 0.75; results not shown). Pulmonary *Saa3* mRNA levels dose dependently increased, and we did not observe any statistically significant differences between the two studied NPs.

Hepatic *Saa*1 mRNA levels increased in a dose-dependent manner 24 h after exposure for both TiO_2 NPs, and only the highest dose was statistically significantly increased compared with the vehicle control (Figure 5). After 3 days, hepatic *Saa1* levels were statistically significantly increased for the two highest doses of NRCWE-001 but not for NRCWE-002. No effects were observed at Day 28. There was no statistically significant difference between the two studied NPs.

Discussion

It has been discussed whether the surface charge of NMs is critical for the biological interactions of NMs (38,39). It has been suggested that positively charged NMs bind to cell surfaces and are taken up by cells more efficiently (40–42). We investigated the inflammatory and genotoxic response of two TiO_2 NPs at 3 doses (18, 54 or 162 µg/mouse) and 3 time points (1, 3 and 28 days post-exposure) following i.t. NRCWE-002 was surface modified exposing amino groups and consequently has a positive zeta potential, whereas NRCWE-001was used as delivered from the supplier. NRCWE-001 is an unmodified rutile TiO_2 and has a negative zeta potential at physiological pH, reflecting an overall negative surface charge presumably caused by the polarity in the crystal structure of the metal oxide. The NRCWE-002 has been reported to induce more DNA damage than NRCWE-001 in HK-2 human kidney cells *in vitro* (43). The two TiO_2 NPs were equally cytotoxic and marginally damaged the hepatoblastoma C3A cell line in humans (33,34). In a recent study, the global gene expression in mouse lung was very similar for NRCWE-001 and -002 (3). In general, the pulmonary transcriptional responses to the two TiO_2s were more similar to each other than to other TiO_2 NPs and TiO_2-containing paint dusts (3).

In this study, inflammation, determined as the influx of neutrophils, was time- and dose dependent and persisted at the highest instilled doses 28 days post-exposure for both NPs. We detected no statistically significant differences in BAL cell numbers for the two TiO_2 NPs. Similarly, pulmonary cellular damage as determined by increased protein concentration in BALF was not statistically different for NRCWE-001 and NRCWE-002.

The TiO_2 NPs are likely to be cleared slowly from lung and to translocate and accumulate slowly (<1% of the instilled dose) in the liver during the 28 days as we have reported previously with another TiO_2 NP (10,11). Both NRCWE-001 and -002 induced increased DNA strand break levels across time points, doses and tissues. BothTiO_2 NPs induced increased DNA strand break levels in lung tissue at all doses 1 and 28 days post-exposure, and NRCWE-002 also increased DNA strand break levels at the low and middle

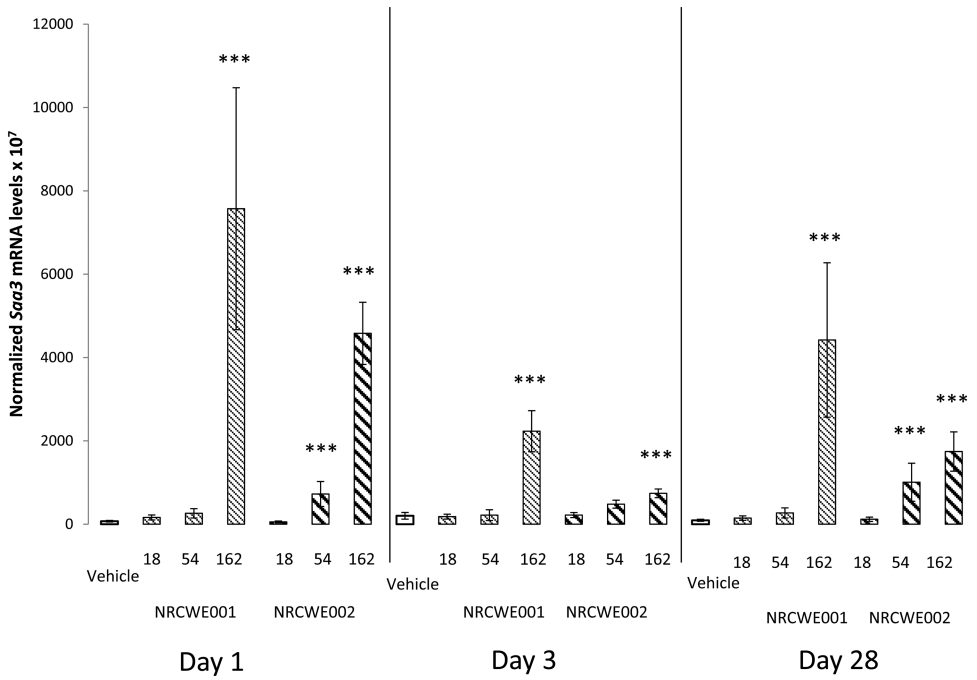

Figure 4. Pulmonary *Saa3* mRNA expression levels with dose response effect in mice 1, 3 and 28 days after intratracheal instillation of NRCWE-001 and NRCWE-002. *Saa3* mRNA levels were normalized to *18S* RNA. The values represent mean of all animals in group ± SEM (n = 8–12). ***P < 0.001: *Saa3* mRNA expression level in TiO_2 NP-treated group vs. vehicle controls.

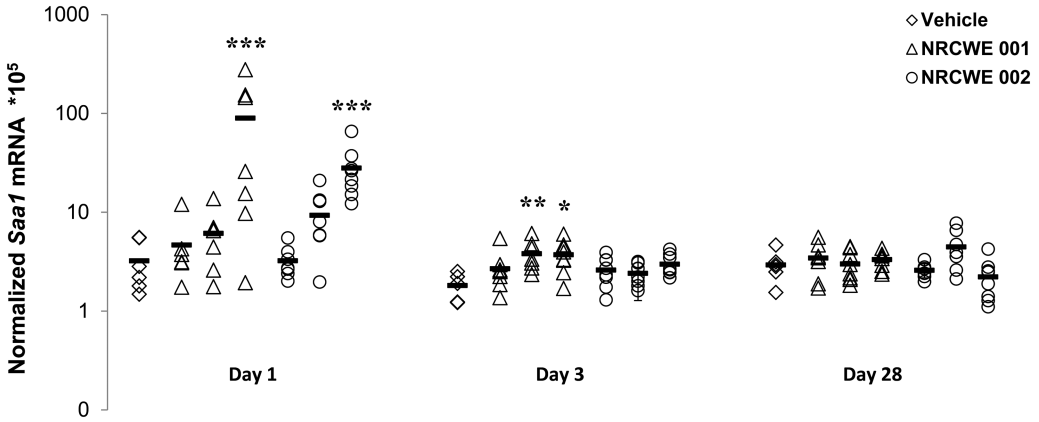

Figure 5. Hepatic *Saa1* mRNA expression levels with dose response effect in mice 1, 3 and 28 days after intratracheal instillation of NRCWE-001 and NRCWE-002. *Saa1* mRNA levels were normalized to *18S* RNA. The values represent mean of all animals in group ± SEM (n = 8–12). *P < 0.05, **P < 0.01, ***P < 0.001: *Saa1* mRNA expression level in TiO_2 NP-treated group vs. vehicle controls.

dose 3 days post-exposure. Importantly, there was no statistically significant difference between genotoxicity in lung tissue for the two TiO_2 NPs. The DNA strand break levels were statistically significantly different for NRCWE-001 and -002 for liver and BAL cells, but no consistent pattern was observed. The statistically significant difference between NRCWE-001 and NRCWE-002-induced BAL cell genotoxicity was likely driven by the lowered DNA strand break levels observed for NRCWE-002. However, NRCWE-002 also induced increased DNA strand break levels in BAL cells (at the highest dose on Day 3 post-exposure). There is no plausible biological explanation for the variation between the materials and over time, and therefore, we believe this is a chance finding. In liver, NRCWE-002 increased DNA strand break levels on Day 1, whereas NRCWE-001 increased DNA strand break levels on Day 3 and Day 28 post-exposure. We doubt that there is any biological explanation for the observed differences in the hepatic NRCWE-001 and NRCWE-002-induced increased levels of DNA strand breaks across doses and time points, and we consider this a chance finding. However, we only assessed DNA damage as DNA strand breaks in the comet assay, and it is possible that the genotoxic potential for NRCWE-001 and -002 may differ for other types of DNA damage.

The variation in DNA strand break levels over time indicates that the level of strand breaks was greater on Day 1 and Day 28 than on Day 3. Actually, we have previously made similar observations following i.t. of carbon black NPs (15,30), diesel exhaust particles (31) and, to a lesser extent, carbon nanotubes.(44) We have no biological explanation for this, but we have observed similar time-dependent variation in the global pulmonary transcription pattern following

i.t. of carbon black NPs (10). It is therefore possible that the time-dependent variation in DNA strand break levels may reflect a true biological effect.

Acute phase response is a risk factor for cardiovascular disease (24,45). We have previously shown that pulmonary deposition of NMs leads to dose-dependent induction of pulmonary acute phase response (23,24,26). Serum amyloid (SAA) binds to high-density cholesterol (HDL), and with marked increases, SAA displaces Apo A-I in HDL and becomes the major HDL protein (24,46). HDL-containing SAA is impaired in its ability carry out cholesterol efflux from macrophages. It has been demonstrated that SAA promotes plaque progression in atherosclerosis-prone apolipoprotein E knockout mice (46), and we recently found that i.t. of SAA is capable of doing so as well (Daniel Vest Christophersen et al., unpublished). Pulmonary *Saa3* transcription is used as a biomarker of pulmonary acute phase response (24), whereas hepatic *Saa1* transcription is a biomarker of hepatic acute phase response (47), and induction of acute phase response is used as a biomarker of particle-induced cardiovascular risk (23–25). In the present study, both TiO_2 NPs induced a strong acute phase gene expression in the lung 1 day after exposure and increased *Saa3* expression was observed even after 28 days. Induction of a systemic acute phase response in the liver was observed in terms of increased expression of *Saa1*, the hepatic isoform of *Saa*. However, the hepatic acute phase response was weaker in terms of fold increase and had much shorter duration compared with the pulmonary acute phase response. Thus, at Day 1, the pulmonary *Saa3* expression was increased 106-fold for NRCWE-001 and 64-fold for NRCWE-002, respectively, whereas the corresponding hepatic *Saa1* expression was increased 28-fold for NRCWE-001 and increased 9-fold for NRCWE-002, respectively. We have previously reported strong time- and dose-dependent pulmonary acute phase response that correlate with total deposited surface area of TiO_2 and carbon black NPs and with neutrophil influx in BALF (23,24). Interestingly, an accompanying hepatic acute phase response was observed following i.t. to two different carbon nanotubes (25) and to a much lesser extent after exposure to another TiO_2 NPs (10) and even less after pulmonary exposure to carbon black NPs (28). Taken together, our results may support the notion that pulmonary and systemic acute phase responses constitute a signalling pathway between particle-induced lung inflammation and cardiovascular health effects (24).

We have previously assessed TiO_2 NPs and sanding dust from paint with and without nanoparticles using the same experimental set-up (1–3,10,11,17,48). Pulmonary exposure to TiO_2 NPs and sanding dust induced pulmonary inflammation but no genotoxicity (1). In a screening of sanding dust from different paints with and without NPs, DNA strand break levels were found to depend on the paint matrix rather than on the content of NPs (17). It has been proposed that genotoxicity of TiO_2 may be due to the reactivity of the surface and it producing reactive oxygen species per se or by biochemical and inflammatory cellular responses (49). It seems that substantial change of surface of TiO_2, which includes change from negative to positive charge, did not change the biological effects in mouse lung. It is therefore unlikely that reactive oxygen species generation at the TiO_2 surface is responsible for genotoxicity and inflammation but rather cellular responses are important.

The inflammatory response to the TiO_2 NP exposure in terms of neutrophil influx at Day 1(184 000 and 118 000 for NRCWE-001 and 002, respectively) was very similar to the previously reported response to the same dose of a surface-coated TiO_2 NP [UV-Titan L181 (189 000 neutrophils) (1), Printex90 (129 000 neutrophils) and the diesel exhaust particle NIST1650b (121 000 neutrophils)] using the same experimental set-up (31). At Day 28, significant neutrophil influx was observed for both TiO_2 NPs and carbon black NPs, whereas no neutrophil influx was observed for diesel exhaust particles. There were no statistically significant differences in the BAL cell composition between NRCWE-001 and NRCWE-002. These results are in agreement with previously observed inflammation in lung after i.t. and inhalation in mice and rats (21,50–52).

Overall, of the change or the surface charge, the studied rutile TiO_2 NP did not influence the toxicological response following pulmonary exposure and therefore, at least with this material, change of surface charge did not affect the toxicity of the NM.

Funding

The project was supported by Danish Centre for Nanosafety (grant no 20110092173-3) from the Danish Working Environment Research Foundation.

Acknowledgements

The authors thank Michael Guldbrandsen, Lisbeth Meyer Petersen, Anne-Karin Asp, Elzbieta Christiansen and Lourdes M. Pedersen for excellent technical assistance. Z.K.Y. was substantially involved in sampling during necropsies; data acquisition, analysis and interpretation of all data; statistical analyses; and drafted the manuscript. N.R.J. participated in designing the study and critically reviewed the manuscript. A.T.S. participated in statistical analyses and revised the manuscript. S.B.E. participated in acquisition of protein measurement data and revised the manuscript. P.J.A. participated in acquisition of DNA damage data on Imstar PathFinder™, their interpretation and revised the manuscript. U.B.V. drafted the manuscript. U.B.V. and H.W.A. were substantially involved in designing the study and acquiring the funds; interpretation of data; and revised the manuscript critically. All authors have read and approved the final manuscript.

Conflict of interest statement: None declared.

References

1. Saber, A. T., Jacobsen, N. R., Mortensen, A., *et al.* (2012) Nanotitanium dioxide toxicity in mouse lung is reduced in sanding dust from paint. *Part. Fibre Toxicol.*, 9, 4.
2. Saber, A. T., Jensen, K. A., Jacobsen, N. R., Birkedal, R., Mikkelsen, L., Møller, P., Loft, S., Wallin, H. and Vogel, U. (2012) Inflammatory and genotoxic effects of nanoparticles designed for inclusion in paints and lacquers. *Nanotoxicology*, 6, 453–471.
3. Halappanavar, S., Saber, A. T., Decan, N., *et al.* (2015) Transcriptional profiling identifies physicochemical properties of nanomaterials that are determinants of the in vivo pulmonary response. *Environ. Mol. Mutagen.*, 56, 245–264.
4. Oberdörster, G., Oberdörster, E. and Oberdörster, J. (2005) Nanotoxicology: an emerging discipline evolving from studies of ultrafine particles. *Environ. Health Perspect.*, 113, 823–839.
5. IARC Working Group on the Evaluation of Carcinogenic Risks to Humans. (2010) *Carbon Black, Titanium Dioxide, and Talc*. IARC Press, Lyon, France.
6. Boffetta, P., Soutar, A., Cherrie, J. W., *et al.* (2004) Mortality among workers employed in the titanium dioxide production industry in Europe. *Cancer Causes Control*, 15, 697–706.
7. Ellis, E. D., Watkins, J., Tankersley, W., Phillips, J. and Girardi, D. (2010) Mortality among titanium dioxide workers at three DuPont plants. *J. Occup. Environ. Med.*, 52, 303–309.
8. NIOSH. (2011). *Current Intelligence Bulletin 63: Occupational Exposure to Titanium Dioxide*. DHHS (NIOSH) publication No 2011–160. Department of health and human services, Centers for Disease Control and Prevention, National Institute for Occupational Safety and Health, Washington, DC, USA.

9. Hougaard, K. S., Jackson, P., Jensen, K. A., *et al.* (2010) Effects of prenatal exposure to surface-coated nanosized titanium dioxide (UV-Titan). A study in mice. *Part. Fibre Toxicol.*, 7, 16.
10. Husain, M., Saber, A. T., Guo, C., *et al.* (2013) Pulmonary instillation of low doses of titanium dioxide nanoparticles in mice leads to particle retention and gene expression changes in the absence of inflammation. *Toxicol. Appl. Pharmacol.*, 269, 250–262.
11. Husain, M., Wu, D., Saber, A. T., *et al.* (2015) Intratracheally instilled titanium dioxide nanoparticles translocate to heart and liver and activate complement cascade in the heart of C57BL/6 mice. *Nanotoxicology*, 9, 1013–1022.
12. Creutzenberg, O., Bellmann, B., Korolewitz, R., Koch, W., Mangelsdorf, I., Tillmann, T. and Schaudien, D. (2012) Change in agglomeration status and toxicokinetic fate of various nanoparticles in vivo following lung exposure in rats. *Inhal. Toxicol.*, 24, 821–830.
13. Halappanavar, S., Jackson, P., Williams, A., Jensen, K. A., Hougaard, K. S., Vogel, U., Yauk, C. L. and Wallin, H. (2011) Pulmonary response to surface-coated nanotitanium dioxide particles includes induction of acute phase response genes, inflammatory cascades, and changes in microRNAs: a toxicogenomic study. *Environ. Mol. Mutagen.*, 52, 425–439.
14. Jackson, P., Halappanavar, S., Hougaard, K. S., *et al.* (2013) Maternal inhalation of surface-coated nanosized titanium dioxide (UV-Titan) in C57BL/6 mice: effects in prenatally exposed offspring on hepatic DNA damage and gene expression. *Nanotoxicology*, 7, 85–96.
15. Bourdon, J. A., Saber, A. T., Jacobsen, N. R., *et al.* (2012) Carbon black nanoparticle instillation induces sustained inflammation and genotoxicity in mouse lung and liver. *Part. Fibre Toxicol.*, 9, 5.
16. Mikkelsen, L., Sheykhzade, M., Jensen, K. A., Saber, A. T., Jacobsen, N. R., Vogel, U., Wallin, H., Loft, S. and Møller, P. (2011) Modest effect on plaque progression and vasodilatory function in atherosclerosis-prone mice exposed to nanosized TiO(2). *Part. Fibre Toxicol.*, 8, 32.
17. Saber, A. T., Koponen, I. K., Jensen, K. A., Jacobsen, N. R., Mikkelsen, L., Møller, P., Loft, S., Vogel, U. and Wallin, H. (2012) Inflammatory and genotoxic effects of sanding dust generated from nanoparticle-containing paints and lacquers. *Nanotoxicology*, 6, 776–788.
18. Johnston, H. J., Hutchison, G. R., Christensen, F. M., Peters, S., Hankin, S. and Stone, V. (2009) Identification of the mechanisms that drive the toxicity of TiO(2) particulates: the contribution of physicochemical characteristics. *Part. Fibre Toxicol.*, 6, 33.
19. Geiser, M. and Kreyling, W. G. (2010) Deposition and biokinetics of inhaled nanoparticles. *Part. Fibre Toxicol.*, 7, 2.
20. Shinohara, N., Oshima, Y., Kobayashi, T., *et al.* (2015) Pulmonary clearance kinetics and extrapulmonary translocation of seven titanium dioxide nano- and submicron materials following intratracheal administration in rats. *Nanotoxicology*, 9, 1050–1058.
21. Shi, H., Magaye, R., Castranova, V. and Zhao, J. (2013) Titanium dioxide nanoparticles: a review of current toxicological data. *Part. Fibre Toxicol.*, 10, 15.
22. Duffin, R., Tran, L., Brown, D., Stone, V. and Donaldson, K. (2007) Proinflammogenic effects of low-toxicity and metal nanoparticles in vivo and in vitro: highlighting the role of particle surface area and surface reactivity. *Inhal. Toxicol.*, 19, 849–856.
23. Saber, A. T., Lamson, J. S., Jacobsen, N. R., *et al.* (2013) Particle-induced pulmonary acute phase response correlates with neutrophil influx linking inhaled particles and cardiovascular risk. *PLoS One*, 8, e69020.
24. Saber, A. T., Jacobsen, N. R., Jackson, P., Poulsen, S. S., Kyjovska, Z. O., Halappanavar, S., Yauk, C. L., Wallin, H. and Vogel, U. (2014) Particle-induced pulmonary acute phase response may be the causal link between particle inhalation and cardiovascular disease. *Wiley Interdiscip. Rev. Nanomed. Nanobiotechnol.*, 6, 517–531.
25. Poulsen, S. S., Saber, A. T., Mortensen, A., *et al.* (2015) Changes in cholesterol homeostasis and acute phase response link pulmonary exposure to multi-walled carbon nanotubes to risk of cardiovascular disease. *Toxicol. Appl. Pharmacol.*, 283, 210–222.
26. Poulsen, S. S., Saber, A. T., Williams, A., *et al.* (2015) MWCNTs of different physicochemical properties cause similar inflammatory responses, but differences in transcriptional and histological markers of fibrosis in mouse lungs. *Toxicol. Appl. Pharmacol.*, 284, 16–32.
27. Hougaard, K. S., Jackson, P., Kyjovska, Z. O., *et al.* (2013) Effects of lung exposure to carbon nanotubes on female fertility and pregnancy. A study in mice. *Reprod. Toxicol.*, 41, 86–97.
28. Bourdon, J. A., Halappanavar, S., Saber, A. T., Jacobsen, N. R., Williams, A., Wallin, H., Vogel, U. and Yauk, C. L. (2012) Hepatic and pulmonary toxicogenomic profiles in mice intratracheally instilled with carbon black nanoparticles reveal pulmonary inflammation, acute phase response, and alterations in lipid homeostasis. *Toxicol. Sci.*, 127, 474–484.
29. Bach, E., Borg, W., Hannerz, H, Lyngby Mikkelsen, K, Melchior Poulsen, O and Tüchsen, F (2002) *Sammenhænge Mellem Arbejdsmiljø og Sygdom/ Erhverv og Hospitalsbehandling som Primær Kilde*. Arbejdsmiljøinstituttet, Copenhagen.
30. Kyjovska, Z. O., Jacobsen, N. R., Saber, A. T., Bengtson, S., Jackson, P., Wallin, H. and Vogel, U. (2015) DNA damage following pulmonary exposure by instillation to low doses of carbon black (Printex 90) nanoparticles in mice. *Environ. Mol. Mutagen.*, 56, 41–49.
31. Kyjovska, Z. O., Jacobsen, N. R., Saber, A. T., Bengtson, S., Jackson, P., Wallin, H. and Vogel, U. (2015) DNA strand breaks, acute phase response and inflammation following pulmonary exposure by instillation to the diesel exhaust particle NIST1650b in mice. *Mutagenesis*, 30, 499–507.
32. Jacobsen, N. R., Møller, P., Jensen, K. A., Vogel, U., Ladefoged, O., Loft, S. and Wallin, H. (2009) Lung inflammation and genotoxicity following pulmonary exposure to nanoparticles in ApoE-/- mice. *Part. Fibre Toxicol.*, 6, 2.
33. Kermanizadeh, A., Gosens, I., MacCalman, L., *et al.* (2016) A multilaboratory toxicological assessment of a panel of 10 engineered nanomaterials to human health-ENPRA project—the highlights, limitations, and current and future challenges. *J. Toxicol. Environ. Health B Crit. Rev.*, 19, 1–28.
34. Kermanizadeh, A., Pojana, G., Gaiser, B. K., *et al.* (2013) In vitro assessment of engineered nanomaterials using a hepatocyte cell line: cytotoxicity, pro-inflammatory cytokines and functional markers. *Nanotoxicology*, 7, 301–313.
35. Jackson, P., Lund, S. P., Kristiansen, G., Andersen, O., Vogel, U., Wallin, H. and Hougaard, K. S. (2011) An experimental protocol for maternal pulmonary exposure in developmental toxicology. *Basic Clin. Pharmacol. Toxicol.*, 108, 202–207.
36. Jackson, P., Pedersen, L. M., Kyjovska, Z. O., Jacobsen, N. R., Saber, A. T., Hougaard, K. S., Vogel, U. and Wallin, H. (2013) Validation of freezing tissues and cells for analysis of DNA strand break levels by comet assay. *Mutagenesis*, 28, 699–707.
37. Saber, A. T., Halappanavar, S., Folkmann, J. K., *et al.* (2009) Lack of acute phase response in the livers of mice exposed to diesel exhaust particles or carbon black by inhalation. *Part. Fibre Toxicol.*, 6, 12.
38. Braakhuis, H. M., Park, M. V., Gosens, I., De Jong, W. H. and Cassee, F. R. (2014) Physicochemical characteristics of nanomaterials that affect pulmonary inflammation. *Part. Fibre Toxicol.*, 11, 18.
39. Karakoti, A. S., Hench, L. L. and Seal, S. (2006) The potential toxicity of nanomaterials: the role of surfaces. *J. Min. Met.Mat. Soc.*, 58, 77–82.
40. Kermanizadeh, A., Balharry, D., Wallin, H., Loft, S. and Møller, P. (2015) Nanomaterial translocation–the biokinetics, tissue accumulation, toxicity and fate of materials in secondary organs–a review. *Crit. Rev. Toxicol.*, 45, 837–872.
41. Zhao, F., Zhao, Y., Liu, Y., Chang, X., Chen, C. and Zhao, Y. (2011) Cellular uptake, intracellular trafficking, and cytotoxicity of nanomaterials. *Small*, 7, 1322–1337.
42. Parak, W. J. (2016) Nanomaterials. Controlled interaction of nanoparticles with cells. *Science*, 351, 814–815.
43. Kermanizadeh, A., Vranic, S., Boland, S., Moreau, K., Baeza-Squiban, A., Gaiser, B. K., Andrzejczuk, L. A. and Stone, V. (2013) An in vitro assessment of panel of engineered nanomaterials using a human renal cell line: cytotoxicity, pro-inflammatory response, oxidative stress and genotoxicity. *BMC Nephrol.*, 14, 96.
44. Poulsen, S. S., Jackson, P., Kling, K., *et al.* (2016) Multi-walled carbon nanotube physicochemical properties predict pulmonary inflammation and genotoxicity. *Nanotoxicology*. 2016 July 7 [Epub ahead of print], doi :10.1080/17435390.2016.1202351
45. Ridker, P. M., Hennekens, C. H., Buring, J. E. and Rifai, N. (2000) C-reactive protein and other markers of inflammation in the prediction of cardiovascular disease in women. *N. Engl. J. Med.*, 342, 836–843.

46. Feingold, K. R. and Grunfeld, C. (2016) Effect of inflammation on HDL structure and function. *Curr. Opin. Lipidol*, 27, 521–530.
47. Saber, A. T., Halappanavar, S., Folkmann, J. K., *et al.* (2009) Lack of acute phase response in the livers of mice exposed to diesel exhaust particles or carbon black by inhalation. *Part. Fibre Toxicol*., 6, 12.
48. Saber, A. T., Mortensen, A., Szarek, J., *et al.* (2016) Epoxy composite dusts with and without carbon nanotubes cause similar pulmonary responses, but differences in liver histology in mice following pulmonary deposition. *Part. Fibre Toxicol*., 13, 37.
49. Knaapen, A. M., Borm, P. J., Albrecht, C. and Schins, R. P. (2004) Inhaled particles and lung cancer. Part A: Mechanisms. *Int. J. Cancer*, 109, 799–809.
50. Park, E. J., Yoon, J., Choi, K., Yi, J. and Park, K. (2009) Induction of chronic inflammation in mice treated with titanium dioxide nanoparticles by intratracheal instillation. *Toxicology*, 260, 37–46.
51. Ma-Hock, L., Burkhardt, S., Strauss, V., Gamer, A. O., Wiench, K., van, R. B. and Landsiedel, R. (2009) Development of a short-term inhalation test in the rat using nano-titanium dioxide as a model substance. *Inhal. Toxicol*., 21, 102–118.
52. van, R. B., Landsiedel, R., Fabian, E., Burkhardt, S., Strauss, V. and Ma-Hock, L. (2009) Comparing fate and effects of three particles of different surface properties: nano-TiO(2), pigmentary TiO(2) and quartz. *Toxicol. Lett*., 186, 152–159.